J Nanostruct 14(2): 492-504, Spring 2024

RESEARCH PAPER

Anticancer Properties of Titanium Dioxide (TiO_2) Nanoparticles Obtained from Quercus infectoria Plant Extract

*Mena Akram Ali *, Saba A. Mahdy, Nehia Neama Hussein*

Division of Biotechnology, Department of Applied Sciences, University of Technology, Baghdad, Iraq

ARTICLE INFO

Article History:
Received 29 January 2024
Accepted 28 March 2024
Published 01 April 2024

Keywords:
Anticancer
Antimicrobial
Antioxidant
Quercus infectoria
TiO_2-NPs

ABSTRACT

The advantages of nanoparticles in the treatments of cancer are rapidly growing, chemotherapy is considered the common treatment for cancer, and radiation and surgery treatment have their disadvantages because it lacks the target of the drug delivery. This study is directing a great deal of attention to TiO_2-NPs that are produced by the methods of green synthesis. These nanoparticles could act as drug transport and carriers and in some cases also as drug replacements for the treatment of cancer. In this study, TiO_2-NPs that are non-toxic and also cost-effective were prepared employing the gall plant extract of *Quercus infectoria*. Green-treated TiO_2-NPs were measured on their purity and were pure; the investigations were carried out through UV–Vis- spectrophotometer, and the diffraction of X-ray (XRD). The analysis of specific and targeting the functional groups responsible for TiO_2-NPs reduction were performed via spectroscopy of Fourier transform infrared (FTIR). Scanning electron microscopy (SEM) was employed to confirm the formation of spherical shapes of TiO_2-NPs.

How to cite this article
Ali M., Mahdy S., Hussein N. Anticancer Properties of Titanium Dioxide (TiO_2) Nanoparticles Obtained from Quercus infectoria Plant Extract . J Nanostruct, 2024; 14(2):492-504. DOI: 10.22052/JNS.2024.02.011

INTRODUCTION

Among the pathogens implicated in urinary tract infections (UTIs), *Staphylococcus epidermidis* and *Staphylococcus haemolyticus*, both Gram-positive bacteria, are notable. While commonly found on the skin and mucous membranes, these organisms can pose a threat, particularly in healthcare settings, where they may exploit compromised immune defenses or the presence of urinary catheters to cause infections. Conversely, *Proteus mirabilis*, a Gram-negative bacterium typically inhabiting the gastrointestinal tract, is recognized as a frequent cause of UTIs, often associated with urinary catheterization or structural urinary tract abnormalities. Notoriously resilient, *P. mirabilis* can instigate stone formation within the urinary tract, necessitating specific antibiotic interventions. In contrast, *Pseudomonas aeruginosa*, a Gram-negative opportunistic pathogen renowned for its adaptability, thrives in diverse environments, including healthcare facilities. Its propensity for causing UTIs is exacerbated in individuals with weakened immune systems or undergoing invasive medical procedures. Combatting *P. aeruginosa* infections proves arduous due to its intrinsic and acquired antibiotic resistance, mandating judicious antimicrobial selection guided by susceptibility testing to ensure effective treatment. The global rise in cancer cases is a growing concern, with individuals diagnosed

* *Corresponding Author Email: as.21.55@grad.uotechnology.edu.iq*

daily. Despite extensive research, new drugs, and numerous studies, exact cancer treatment remains elusive. The continuous increase in cancer cases emphasizes the need for innovative approaches. Nanotechnology is a promising field becoming widely known as a method that shows clear signs of future success in cancer research and treatment, employing nanotechnology in the research of cancer represents a cause of a marked change and approach to address the limitations of treatment. As the need for effective and successful solutions grows and continues to exist, involving nanotechnology in the studies of cancer represents a significant potential frontier [1]. In the sphere of biological sciences: biotechnology and medicine, nanotechnology has gone beyond regular boundaries, venturing into the field of nano-biotechnology. The integration of nanobiotechnology into medicine has been a successful instrument in the current and ongoing improvements of the quality of human life. As a result, nano-medicine has surfaced as a distinct field, allowing researchers and scientists to develop the prevention of disease strategies, and enterprising healthcare measures [2]. It is crucial to embrace the measures of precautions and educate ourselves proactively about the potential in the environment and other pollution issues, as well as the risks of the health-related issues that may come to light from the misemploy of nanotechnology. This is considered of the most importance, stating the growing interest in sustainability worldwide. By combining nanotechnology with the principles of sustainability, the way for a sustainable and promising prospect for this field could be preserved, ensuring that its benefits are realized while minimizing adverse impacts on the environment and living organisms [3]. Nanomaterials is a promising field, offering a wide range of applications especially cancer therapy [4]. Towards the creation of novel anticancer agents, significant investigations have been directed with nanotechnology playing an important role, noting, the majority of interactions between biomaterials and cells transpire at the nanoscale. nanostructures can engage with biomolecules on the cell surface [5]. According to the World Health Organization, there is a projected increase in annual cancer cases, expected to rise from 14 million in 2012 to 22 million by the year 2030 [6]. Most concentrated solution of Ag/TiO_2 nanofibers led to the complete cessation of oral cancer cell proliferation and migration. This exceptional performance is likely attributed to the heightened reactivity of the surface and the level of the interaction between titanium dioxide and silver on an atomic level, accompanied by the silver ions release. These mechanisms collectively underpin the remarkable efficacy of the nanofibers generation**.** The observation of the biological effects underscores the possible utility of silver and titanium nanofibers in both anticancer [7]. Ag/TiO_2 nanoparticles (NPs) exhibited significant generation of reactive species of oxygen (ROS), which ultimately led to the complete suppression of cell growth of cancer upon their systemic in vitro application. Furthermore, the Ag/TiO_2 NPs efficiently absorbed visible light, thereby enhancing their anticancer sensitivity by inducing cancer cell death and inhibiting cell proliferation, as confirmed through cell viability assay testing [8].

The study aimed to evaluate the effect of TiO_2-NPs, obtained through green synthesis, on the viability of HSSCC cells at different concentrations, focusing on concentration-dependent effects over different periods and exploring the MIC properties that reduce biofilm formation isolated from urinary tract infections. TiO_2-NPs when presented as a homogeneous mixture showed strong anticancer potential and produced maximum antioxidant activity, demonstrating a strong and necessary anticancer ability against melanoma cell line, which helped to overcome melanoma cells. The observations indicate that TiO_2-NPs may become an anti-cancer therapeutic treatment in the future.

MATERIALS AND METHODS

Materials

The media utilized included Mannitol Salt aga**r** , MacConkey agar , Muller-Hinton broth (MHB) utilized to anti-biofilm ,Alcoholic ethanol was used in the extraction process of *Q. infectoria plants*. In addition to its use titanium tetra isopropoxide (TTIP) in preparing nanoparticle TiO_2.

Collection of microbial isolated

The study involved gathering form UTI infection acquired in hospital. The diagnosis was established through the examination of the isolates morphological trait via culture media growth. The identified microbes include *s.epidemidis*, *p.mirabilis ,p.aeruginosa ,s.hamolyticuds.*

Preparation of plant extract

Q. infectoria gall underwent a cleaning process by washing with tap water to eliminate the tiny particles of dust from its outer surface. The plants were then cleansed with distilled water and left to dry at room temperature. After complete dryness of the plant at room temperature a fine powder was obtained when transferred and crushed by the grinder. Extraction by Alcohol: by the method described in reference [9] alcoholic extract of the plant was prepared, the extraction was performed by a continuous process in a Soxhlet applying Ethanol as a solvent at eighty percent concentration for seven hours, a further concentration process were carried out using a Rotary Evaporator, then the product were dried using oven at forty Celsius degree and preserved in bottles that were clean and sterilized, the product were kept in refrigerator until utilization.

Green synthesized TiO_2 nanoparticles preparation

The Green synthesized process of TiO_2 nanoparticles was carried out by applying one point six millimoles of Titanium tetraisopropoxide in fifty milliliters of isopropyl alcohol thereafter the addition of twenty-five milliliters of plant extract took place, under continuous mixing at seventy Celsius degree in two hours period. Afterward, the homogeneous mixture is left to age for over twenty-five hours. The obtained yellowish brown liquid was then transferred over hot air and kept at eighty Celsius degrees for eight hours then a dark and dry homogenous material was obtained and then converted to a powder. The acquired powder was rinsed multiple times with DI and ethanol. The resulting product was dried, calcined at three hundred fifty celsius degrees for three hours, ground, and then stored as TiO_2-NPs, a method used with some modifications [10].

Characterisation of TiO_2 nanoparticles

The analysis of X-ray diffraction on the produced powder was performed via (XRD Shimadzu-Japan). The characterization of Titanium dioxide nanoparticles's morphology was performed by Scanning electron microscopy (SEM) to determine the shape and size of these nanoparticles. It was subjected to a Scanning Electron Microscope (Zeiss, Jena, Germany). The spectra over the range of 400 - 4000 cm^{-1} were recorded employing a Fourier Transform Infrared device (FTIR Shimadzu-Japan). Finally, TiO_2 nanoparticles were characterized using a UV-Vis spectrophotometer (Chrom Tech, USA).

Anticancer Activity

Preparation of Cancer Cell Lines

The cytotoxic impact of TiO_2-NPs, the experiment was conducted to investigate the toxic effects of test substances at concentrations (0.0, 1.95, 3.9, 7.8, 15.62, 31.25, 62.5, 125, 250, 500, 1000 µg/mL) on a HSSCC line in passage 27. The cells were cultured in RPMI-1640 medium supplemented with 10% Fetal Calf Serum (FCS). The cytotoxic impact of the test substance was examined by culturing cells in multiwell tissue culture plates (96-Microtiter plates) with a flat bottom. The experiment consisted of three stages: Cells Seeding: After activating and proliferating cancer cell lines for 24 hr, the monolayer growth was treated with Trypsin-Versen solution. Subsequently, 25 mL of RPMI-1640 medium, prepared with serum, was added to each well, adjusting the cell count to 1x104 using a counting chamber. A volume of 100 µl of the cell suspension was distributed into the tissue culture wells, which were then incubated at 37 °C for 24 hr to allow cell attachment to the glass [11].

Preparation of different TiO_2-NPs concentrations

Different concentrations of the test substance were prepared using a serum-free tissue culture medium. These concentrations were added to the wells containing adherent cancer cells, and solutions were prepared just before use. Six replicates were used for each treatment. The culture medium in the plates was poured out, designating column 1 as the negative control, to which 200 µl of serum-free culture medium was added. Columns 2 to 12 received increasing concentrations (200 µl per well) of the test substance. The plates were covered, incubated at 37°C, and exposed for different durations (24, 48, 72 hrs).

Minimum Inhibitory Concentration

Microtiter Plate Method

The antibacterial activity of was assessed using minimum inhibitory concentration MIC assays against Gram-negative s.*haemolyticus*, *sepidermids*, *p.mirabilis*,and *p.aeruginosa* [12] Stated that the MIC was determined on a 96-well microtiter plate using the resazurin assisted microdilution technique in Mueller-Hinton broth

(MHB) as follows:
1. Test material, which was: Plant extract (*Q.infectoria)*, and TiO_2 nanoparticle.
2. Preparation of test materials with triple the final required concentration.
3. 100 µl of broth medium in each well from 1 to 10 were made.
4. 100 µl of diluted test material was transferred to the first well. by transferring 100 µl from the first to the 10th well (the concentrations were 100, 50, 25, 12.5, 6.25, 3.12, 1.56, 0.78, 0.39, and 0.19 µg/ml) in addition to the controls.
5. Each well was inoculated with 100 µl of bacterial suspension equivalent to McFarland standard no 0. 5 (1.5 ×10 8 CFU\ml).
6. The microtiter plate was incubated at 37 C for 24 h. 8- 30 µl of resazurin (0.015%) prepared in ((3.2.5.5) was added to each well (30 µl/well), and incubated for 2 to 4 hrs. for the observation of color change. After completion of the incubation, rows with no color change (blue resazurin color remained unchanged) were scored as above the MIC whereas the last blue well in the row recorded as MIC.

Anti-biofilm

The microtiter plate (MTP) assay is a qualitative technique that uses a microplate reader to determine an agent's effectiveness against biofilm formation. The minimum inhibition concentrations MIC obtained from the previous experiment were used to study the effect of the test materials on the formation or inhibition of biofilm of the studied s.*haemolyticus*, *sepidermids*, *p.mirabilis*,and *p.aeruginosa* isolates that produce strong biofilm, the test materials were: Plant extraction (*Q.infectoria),* and TiO_2 NPs.

The same previously mentioned protocol (MTP) was used for the biofilm formation assay. However, 100 µl of test compounds was added. the plate was incubated at 37 °C for 24h. After that, all wells were washed, stained, and read at 600 nm wavelength using a micro-plate reader. percent of biofilm inhibition was calculated by the equation 1 [13].

Cytotoxicity Assay of TiO_2-NPs

After the designated incubation duration, the contents of the plates (cell sediment, culture medium) were discarded, and wells were cleaned three times with phosphate-buffered saline to remove any traces of the TiO_2-NPs and unattached cells. Then, ten micro-litters of MTT dye solution (final concentration 0.5 mg/ml) were added to each well and left for 4 hours at 37 ℃ in a CO2 incubator. The cells underwent a multiple times

$$\% \text{ Biofilm inhibition} = [(\text{OD Control- OD Sample})/\text{OD Control}] \times 100 \quad (1)$$

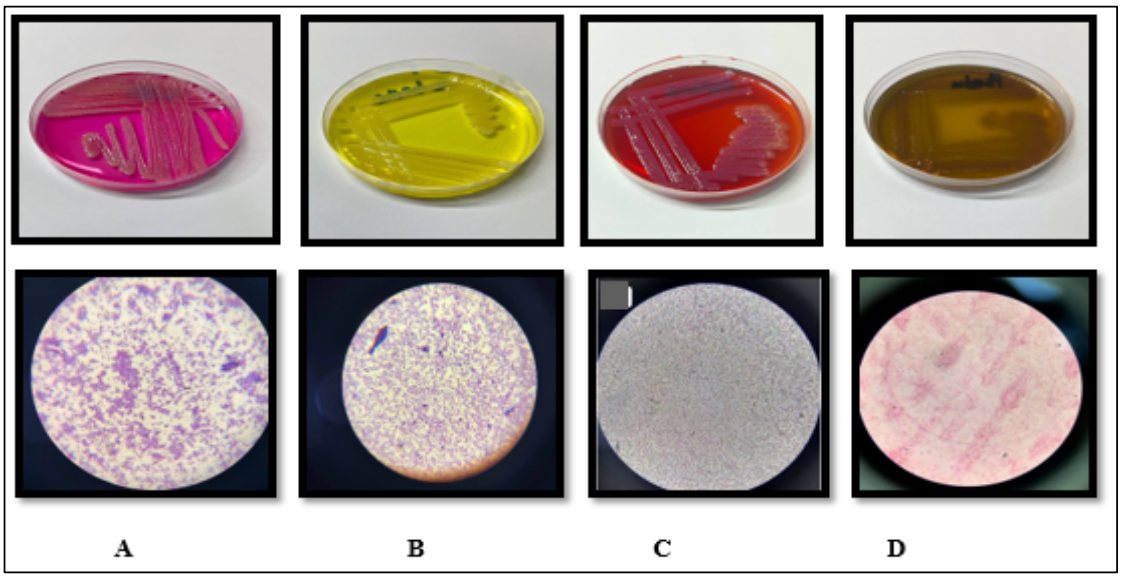

Fig. 1. Culturing and Microscopic Examination (A) *s.epidermidis* (B),*s.haemolyticus* ,(C) *p.mirabils*(D),*p.aeruginosa.*

cleaning process with phosphate-buffered saline until any surplus dye was eliminated. After complete drying of the plates, 100 µl of DMSO was added to ensure complete dissolution of the violet formazan crystals. The outcomes were interpreted through an ELISA microplate spectrophotometer employed at a wavelength of 500 nanometers for result analysis. The inhibitory rate was determined using the equation 2 [14].

Antioxidant

The method mentioned in (Brand-Williams et al, 1995) was followed in conducting the antioxidant antioxidant test, using the method (2, 2-diphenyl-1-picryl-hydrazylhydrate DPPH), by adding 0.024 grams of DPPH to 50 milliliters of absolute ethyl alcohol. It is dissolved well by mixing it on a magnetic stirrer without heat, then the volume is supplemented to 100 milliliters with absolute ethyl alcohol to give a final concentration equal to 0.024 mg/ml. Then, half a milliliter of serial concentrations of the test substance (0.0, 25, 50, 100, 150, 200) µg/mL were taken and added to a mixture of DPPH (0.5.) mM and mL (3.3) of absolute ethanol. The amount of color change was measured using The spectrophotometer was at a wavelength of 515 nm during 100 minutes of reaction at room temperature. The plank tube contained (3.3) mL of absolute ethanol and (0.5) mL of the sample, and the control tube contained (3.3) mL of absolute ethanol. And (0.5 mL) of DPPH. The removal percentage was calculated according to the equation 3.

Ascorbic acid or vitamin C at a concentration of 1/1 (1 mg/100 ml of distilled water) is used as a positive control due to its high effectiveness as an antioxidant and is considered a standard material for comparison.

Statically analysis

The one-way analysis of variance (ANOVA) and subsequent post-hoc tests were conducted using IBM SPSS Statistics for Windows, version 26 (SPSS Inc. Chicago, Illinois, United States). Variables were expressed as mean ± standard deviation (SD). The level of significance was set at $p \leq 0.05$.

RESULTS AND DISCUSSION

In the present study, all isolates were examined primarily for colony characterization by culturing on the selective media, Mannitol salt , MacConkey agar incubated for 24 hours at 37ºC. The appeared colonies of *s.epidermidis* on Mannitol salt results

$$\text{Inhibitory Rate} = (1 - \text{Absorbance of the test substance} / \text{Absorbance of the negative control}) \times 100 \quad (2)$$

$$\text{Antioxidant Activity} = 100 - \frac{1 - \text{sample absorbency}}{\text{control absorbency}} \times 100 \quad (3)$$

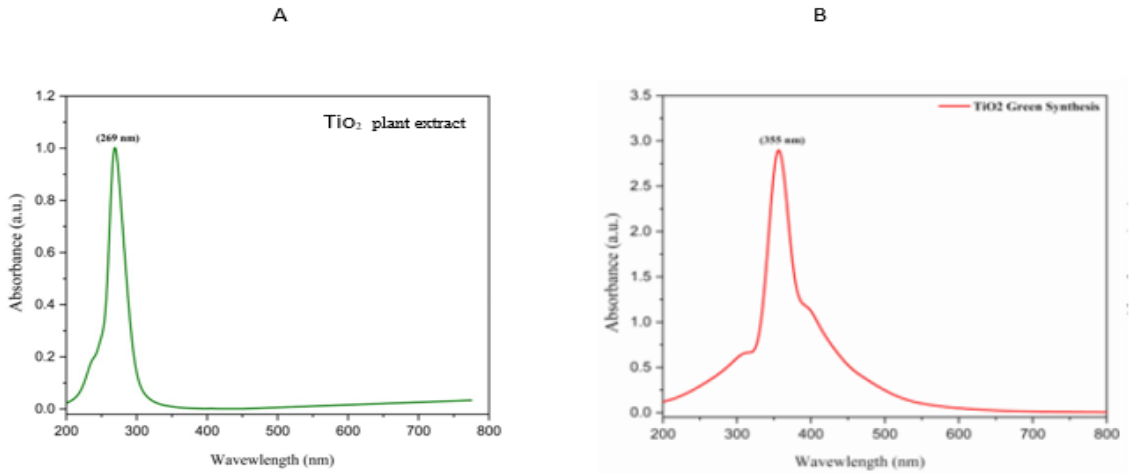

Fig. 2.A- UV absorption of the plant extract, B-UV absorption of TiO_2-NPs obtained by green synthesis.

growth of mucoid metallic pink colonies which refer to the presence of *s.epidermidis* . and appeared yellow colonies on mannitol salt which refer to the presence of *s.haemolyticus* .On MacConkey agar, red, mucoid, lactose fermented colonies were considered mirabilis. while colonies on Mackonky, brown , mucoid, colonies which refer to the presence of *p.aeruginosa* Fig. 1. In addition gram staining and microscopic observation were carried out for all isolates to determine the cell size, color and form and as shown in the Fig. 1 below. spherical or sub-spherical shape budding yeast-like cells Gram-positive bacteria stain violet because of the crystal violet assay when seen

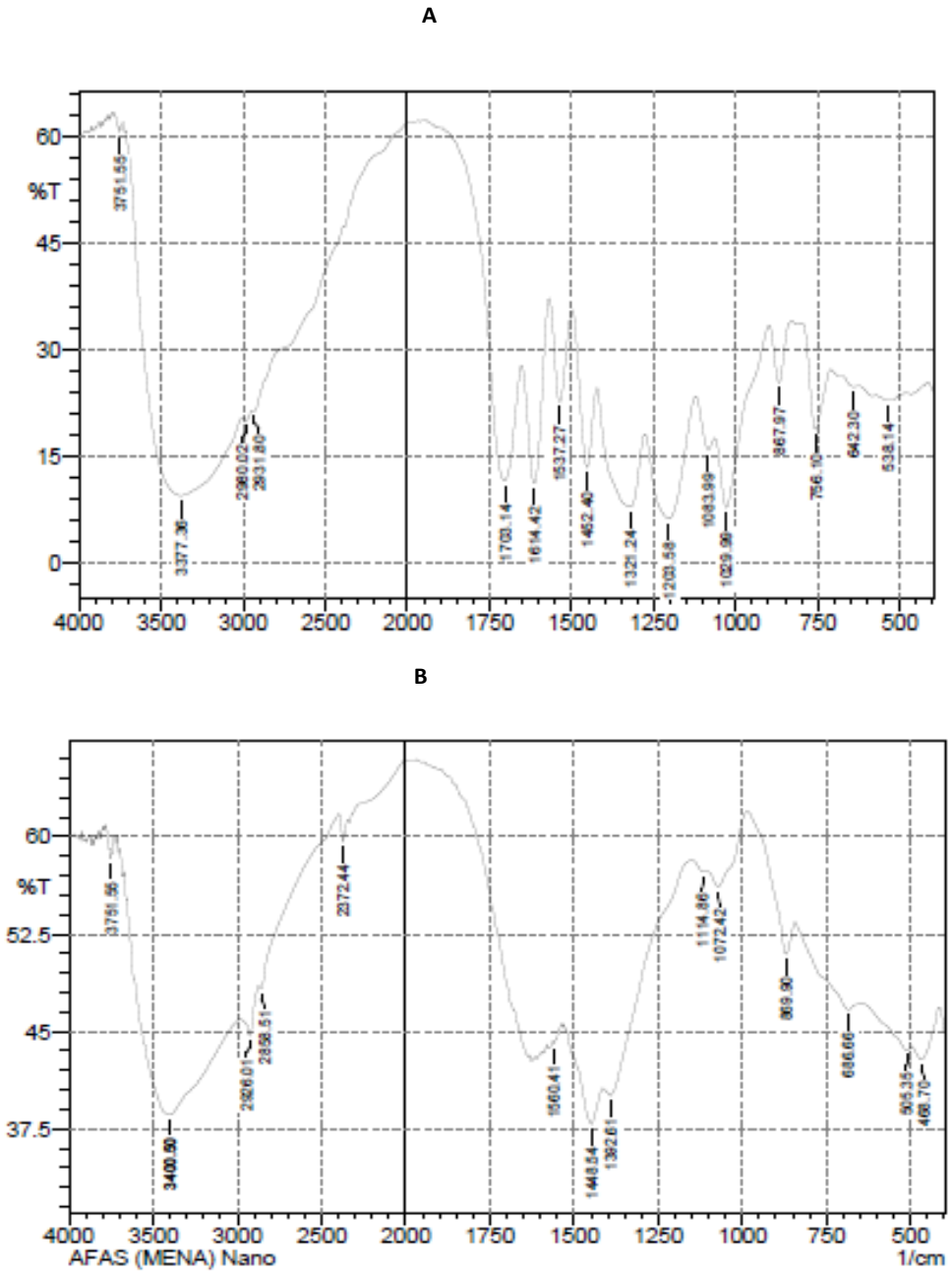

Fig. 3.A-FTIR of plant extract, B-FTIR of green synthesized TiO_2.

with a light microscope. This pigmentation is due to the peptidoglycan layer of the cell wall. On the other hand, gram-negative bacteria do not lag behind the crystal violet stain, because they absorb counter stain (safranin) and appear pink or red due to a layer of peptidoglycan layer that is thinner and confined between the outer and inner envelope of the cell.

Fig. 2 (A) depicts the optical absorption spectrum of plant extract with absorption notably centered around 269 nm. On the other hand Figure 1 (B) shows illustrates the optical absorption spectrum of green synthesized TiO_2-NPs. Notably, the absorption edge is centered on 355 nm. To assess the suitability of the manufactured materials for various applications, it is crucial to compute the band gaps. The Tauc plot method was employed for the band gap measurements of the synthesized TiO_2-NPs. This analytical approach aids in understanding the electronic properties of

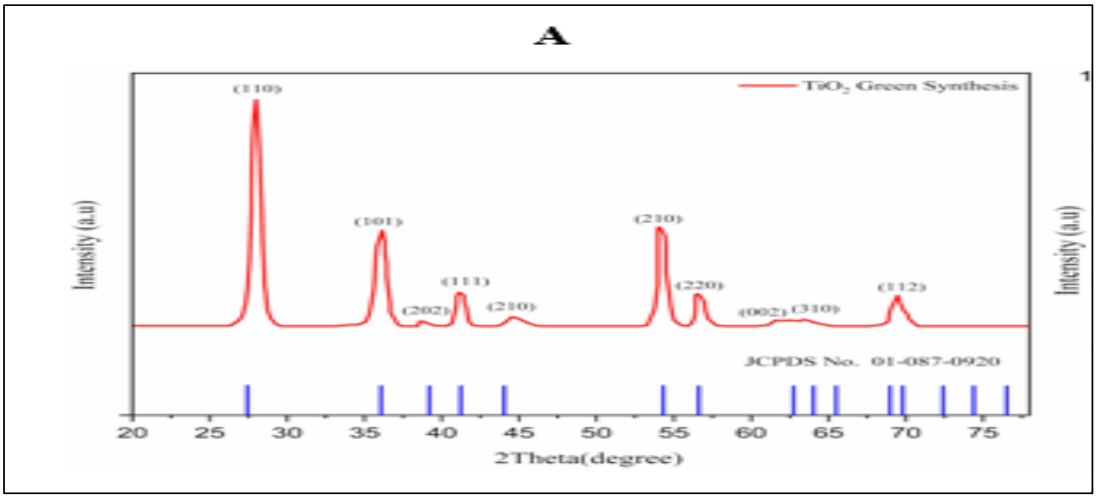

Fig. 4. A-The X-ray diffraction (XRD) profile of TiO_2 nanoparticles obtained by green synthesis method.

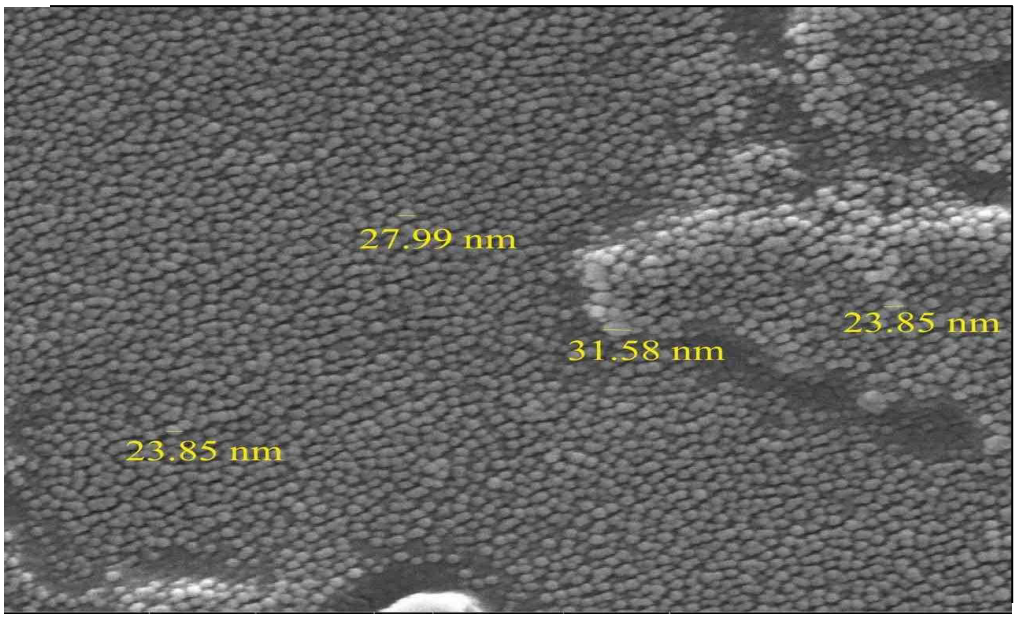

Fig. 5. Displays scanning electron microscope (SEM) micrographs of TiO_2-NPs obtained by green synthesis method.

the nanoparticles and is essential for evaluating their potential utility in diverse applications.

Fig. 3A illustrates the spectrum of FTIR of plant extract, nanoparticles versus green synthesized TiO_2 (Fig. 3B). However, in Fig. 3A, the peaks align with 3377.36 cm^{-1}. In spectra, the observed peaks result from the stretching of hydrogen bonds in the hydroxyl functional group, O-H (alcohol) group. Peaks at 2980.02 cm^{-1} were identified as the C-H (alkane stretching and -C≡C-(alkynes ,lack of positional isomerism in symmetrical alkynes) functional group functional group. The spectrum of FTIR of TiO_2 nanoparticles had peaks matching 3400.24 cm^{-1}, in the spectra because of the

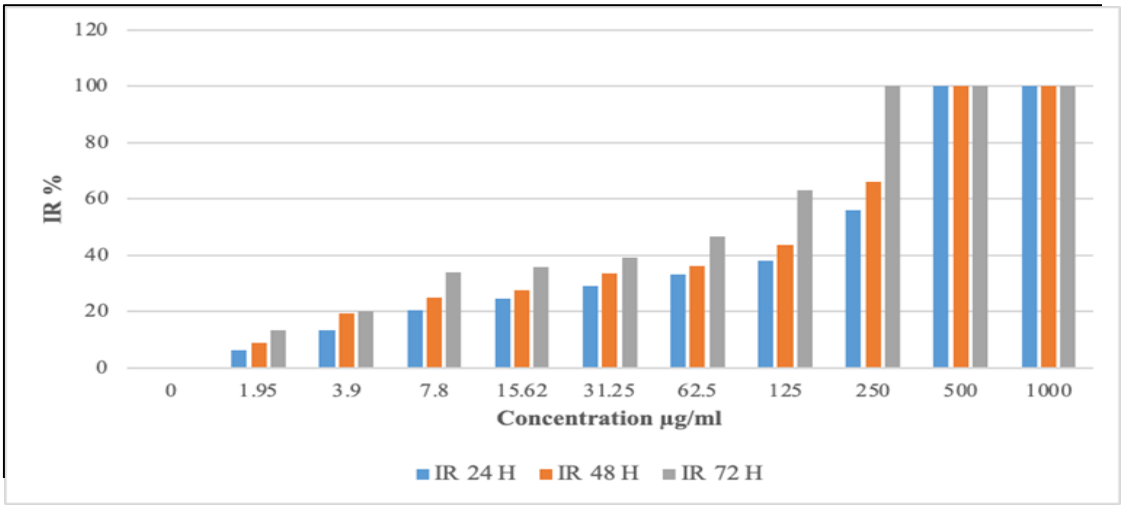

Fig. 6. Inhibition rate (IR) of Plant Extract on HSSCC Cells after Different Exposure Duration.

Table 1. Effects of different concentrations of plant extract on Human skin Squamous Cell Carcinoma (HSSCC), after 24, 48, and 72 hours of exposure.

Concentration (µg/mL)	Plant extract			*P* value
	24 h (N=2)	48 h (N=2)	72 h (N=2)	
0	1.77 ± 0.01 a	1.78 ± 0.01 a	1.84 ± 0.05 a	0.22
1.95	1.72 ± 0.01 a	1.75 ± 0.01 a	1.72 ± 0.01 a	0.21
3.9	1.70 ± 0.00 a	1.71 ± 0.01 a	1.70 ± 0.00 a	0.09
7.8	1.67 ± 0.01 a	1.69 ± 0.01 a	1.63 ± 0.01 b	0.02
15.62	1.66 ± 0.01 a	1.64 ± 0.01 ab	1.61 ± 0.01 b	0.03
31.25	1.60 ± 0.02 a	1.58 ± 0.03 a	1.53 ± 0.03 a	0.17
62.5	1.55 ± 0.01 a	1.51 ± 0.01 ab	1.46 ± 0.03 b	0.04
125	1.44 ± 0.03 a	1.42 ± 0.03 a	1.41 ± 0.01 a	0.43
250	1.41 ± 0.00 a	1.40 ± 0.00 a	1.34 ± 0.01 b	0.01
500	1.34 ± 0.06 a	1.33 ± 0.04 a	1.31 ± 0.01 a	0.71
1000	1.30 ± 0.00 a	1.25 ± 0.05 a	1.21 ± 0.01 a	0.12

Distinct lowercase letters indicate noteworthy variances, while comparable lowercase letters indicate insignificance.

stretching of the hydrogen bond of the hydroxyl O - H group (Alcohol), the peaks equivalent to 2926.01 cm-1 was displayed as the C-H Functional group of (alkane stretching and - C≡C-(alkynes ,variable not present in symmetrical alkynes). Peaks marked at 1448.54 cm^{-1} are for C = C (medium weak multiple bands). Functional group of (alkane stretching and - C≡C-(alkynes ,variable not present in symmetrical alkynes).

Fig. 4 illustrates the X-ray diffraction (XRD) patterns of TiO_2-NPs. The distinctive creation of rutile-phase TiO_2 nanoparticles is evident in the patterns. The diffraction peaks angles (2θ) = 28, 36.14, 38.83, 41.13, 44.55, 54.03, 56.52, 61.81, 63.43 and 69.47 correspond to the lattice planes of (110), (101), (202), (111), (210), (220), (002), (310), and (112), respectively (JCPDS no. 01-087-0920). To determine the crystallite sizes of TiO_2 nanoparticles, Scherrer's equation.Utilizing a Scanning Electron Microscope (SEM) for the examination of nanoparticle morphological characteristics, the Field Effect Scanning Electron Microscopy is employed. In Fig. 5, SEM micrographs of TiO_2 nanoparticles at 120,000X magnification are presented for reference. The images showcase sphere-like structures, SEM This visual data enhances understanding of structural characteristics, representations reveal minimal aggregation in TiO_2-NPs, providing valuable insights into their morphology distribution validated through comparison with relevant literature on TiO_2-NPs

Various concentrations of the extract were employed, and the viability of HSSCC cells was measured after 24, 48, and 72 hours of exposure. The summarized findings are presented in Table 1. Observing Table 1 it could be assumed that the starting concentration point of the concentration was 7.8 µg/mL the HSSCC viability started gradually drooping after 24 and 72h of incubation with plant extract. 24-Hour Exposure: At a concentration of 0 µg/mL, cell viability was (mean ± SD; 1.77 ± 0.01). As the concentration increased, no significant differences were observed within this time frame ($p > 0.05$). The p-value for the overall effect was 0.22. 48 Hours Exposure: Similar to the 24-hour exposure, no significant differences were observed between concentrations ($p > 0.05$) at the beginning of the 48-hour exposure. The p-value for the overall effect remained non-significant at 0.21. 72 Hours Exposure: Table 1 represents the effects of plant extract concentrations on HSSCC cells at different time durations 24, 48, and 72 hours, while Fig. 6 represents the inhibition rate of plant extract. Concentration levels were divided into control (0 µg/mL) which serves as the baseline control group with no treatment, low concentrations (1.95 µg/mL, 3.9 µg/mL, and 7.8 µg/mL) representing the lower end of the dose range, intermediate (15.62 µg/mL, 31.25 µg/mL and 62.5 µg/mL) these concentrations cover the mid-range of doses and a higher concentrations (125 µg/mL, 250 µg/mL, 500 µg/mL and 1000 µg/mL) these concentrations represent the higher end of the dose range. At 24 hours of exposure, the inhibition rates (mean ± standard deviation) of plant extract on HSSCC cell viability were observed. assessing the impact of plant extract on HSSCC cell viability. After 72 hours of exposure, significant differences were observed in cell viability at varying concentrations. At 0 µg/mL and 1.95 µg/mL concentrations, the viability was significantly different from the other concentrations. At the highest concentration of 250 µg/mL, cell viability was significantly lower compared to other concentrations. The overall effect was statistically significant with a p-value of 0.01. The impact of the obtained plant extract on HSSCC cell activity and viability changes depending on the duration of exposure and the concentration of the dosage were the main results of this study indicated that after 72 hours of exposure, significant differences in cell viability at various concentrations was observed, higher cell viability was observed with the lower concentrations and vice versa, reduced viability at the high concentrations. Therefore, the dose-dependent effect of the plant extract on the activity of HSSCC in a certain period would be suggested. Furthermore, it could be concluded that TiO_2-NPs have concentration-dependent effects on the viability of HSSCC cells. Obtained results provide valuable insights into the possible employment of these nanoparticles and plant extract as a therapeutic agent against cancer and specifically HSSCC, however, the mechanism of action and safety should be further investigated. Torres et al. (2016) conducted a study on the impact of α/β-thujone on glioblastoma, using both models *in vitro and in vivo*. They found that α/β-thujone possesses the capacity to reduce the feasibility of a cell and exhibits anti-proliferative, pro-apoptotic, and anti-angiogenic characteristics in vitro.

On the other hand, In the studies conducted

in living organisms, α/β-thujone was observed to prompt regression of neoplasia and inhibit markers related to angiogenesis such as CD31, Ang-4 and VEGF within the tumor [15]. The antitumoral efficacy of the *Q. infectoria* extract has been assessed across various cancer cell lines [16-19]. These studies collectively contribute to our understanding of the potential anticancer

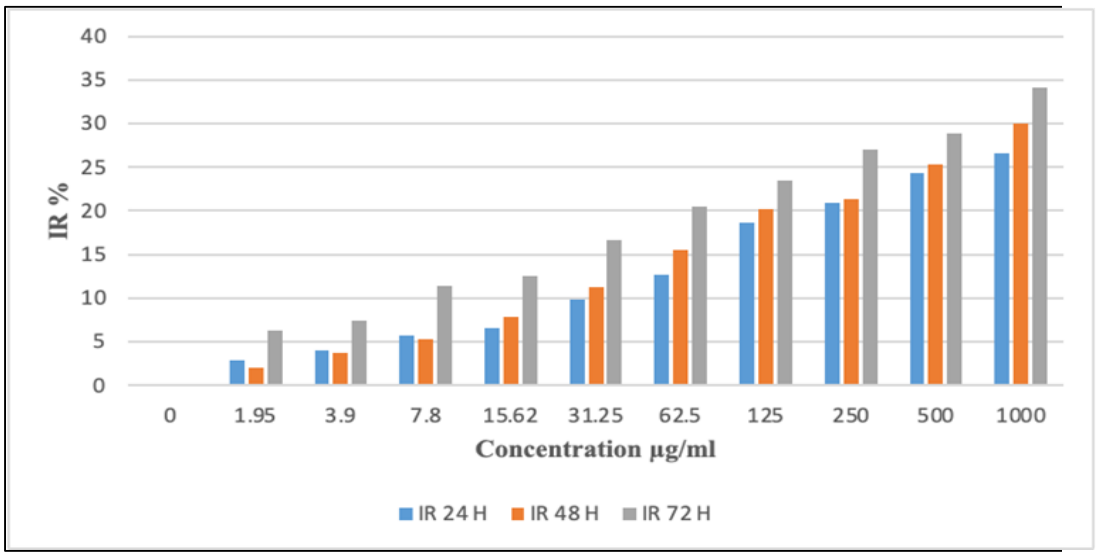

Fig. 7. Inhibition rate (IR) of TiO_2-NPs on HSSCC Cells After Different Exposure Duration.

Table 2. Effects of different concentrations of green synthesized TiO_2-NPs on HSSCC, after 24, 48, and 72 hr of exposure.

Concentration (µg/mL)	TiO_2-NPs			*P* value
	24 h (N=2)	48 h (N=2)	72 h (N=2)	
0	1.85± 0.01 a	1.87 ±0.00 b	1.88± 0.00 b	0.01
1.95	1.73± 0.01 a	1.70± 0.00 a	1.63± 0.05 b	0.01
3.9	1.60± 0.00 a	1.51± 0.01 b	1.50± 0.00 b	0.00
7.8	1.47± 0.01 a	1.41± 0.01 a	1.24± 0.03 b	0.00
15.62	1.39± 0.03 a	1.36± 0.01 a	1.21 ±0.01 b	0.00
31.25	1.31± 0.01 a	1.24± 0.06 ab	1.14 ±0.01 b	0.04
62.5	1.24± 0.02 a	1.20± 0.02 a	1.00± 0.01 b	0.00
125	1.14 ±0.05 a	1.05 ±0.07 a	0.70± 0.02 b	0.01
250	0.81± 0.01 a	0.64 ±0.03 b	0.00± 0.00 c	0.00
500	0.00± 0.00	0.00± 0.00	0.00 ±0.00	__
1000	0.00± 0.00	0.00± 0.00	0.00± 0.00	__

properties associated with the use of *Q. infectorias* in homeopathic treatments.

On the other hand, Table 2 and Fig. 7, demonstrate the different concentrations of TiO_2-NPs on HSSCC viability: The control (0 µg/mL): This serves as the baseline control group with no treatment. It helps you compare the effects of the treatment groups to the untreated cells. Low Concentrations (7.8 µg/mL, 3.9 µg/mL, and 1.95 µg/mL): These concentrations represent the lower end of your dose range. You might expect minimal or no effects on cell viability or proliferation at these levels. Intermediate Concentrations (62.5 µg/mL, 31.25 µg/mL, and 15.62 µg/mL): These concentrations cover a mid-range of doses. Effects on cell viability and proliferation may become more pronounced at these levels. Higher Concentrations (1000 µg/mL, 500 µg/mL, 250 µg/mL, and 125 µg/mL): These concentrations represent the higher end of your dose range. You may anticipate more significant effects on HSSCC cells at these concentrations, including potential cytotoxicity or inhibition of cell growth. Surprisingly all the examined concentrations were cider to the HSSCC and the viability in almost all concentrations was significantly decreasing.

MIC plant extract the result t of Table 3 the minimum inhibiter concentration plant extract were are identical for three pathogen isolated *p.mirabilis* however a lower minimum inhibiter contraction were deducted when *s.haemolyticus* was tested given 3.12 mg/ml. MIC of green synthesis TiO_2 were identical the three pathogenic namely *s.epidermidis* , *S.haemolyticus , p.mirabilis* given concertation of 50 mg/ml will the concentration 25 was the MIC of the *p.aeruginosa* and this was the lower MIC among the green synthesis TiO_2 and the rest of the all tested plant

Table 3. MIC of bacterial pathogen of plant extract and ,TiO_2 NPS.

bacteria	Plant extract mg/mL	Tio_2 green synthesis mg/mL
s.epidermidis	12.5	50
s.haemolyticus	3.12	50
p.mirabilis	12.5	50
p.aeruginosa	12.5	25

Table 4. Effect of plant extract *Q.infectoria*, TiO_2 NPs of four sample isolates of bacteria.

isolates	Control	*Q.infectoria*	Tio_2 NPs
s.haemolyticus	100%	86.1%	100%
s.epidermidis	100%	19.7%	75.1%
p.mirabilis	100%	47.6%	83.9%
p.aeruginosa	100%	45.5%	100%

Table 5. Antioxidant activity of green synthesized TiO_2-NPs and Plant extract.

Parameters	Concentration µg/mL	Antioxidant activity %
Tio_2-NPs	0.0	0.0
	25	16.30
	50	24.45
	100	37.59
	150	50.0
	200	64.16
Plant extract	0.0	0.0
	25	12.65
	50	21.89
	100	35.88
	150	46.71
	200	61.55

extract and TiO_2 nanopartical. Where the results shown in the Table 3 indicated that the types of interactive oxygen (ROS), along with free radicals, produce the TiO_2 which has damaged the wall of bacterial cells and also prevents respiratory enzymes.

Biofilms are accumulations of bacteria that are adhered to the surfaces and embedded in a self-produced matrix. The matrix of biofilm contains substances, such as proteins ,polysaccharides, and extra-cellular DNA, which protect bacteria from harsh environmental conditions and provides resistance to human immunity. The film can also withstand a variety of chemotherapeutic agents. Since infections produced by bacteria that form a biofilm are hard to treat, there is a need to search for new and novel biofilm inhibitors . In this study, the ability of, *S.epidermids* , *S.hoemolyticus* ,*p mirobilis* and *P aeruginasa* isolates to form biofilm was tested using a Microtiter plate (MTP) and read by Microtiter spectrophotometer. The results showed that there are some isolates that adhere and are able to produce biofilm while others are non-adherent and unable to form biofilm. as shown in the Table 4 in use condition plant extract There is *s.epidermidis* isolates that are strong for biofilm however ,in the case of used TiO_2 (green synthesis) moderate biofilm four isolates of , *S.aeruginosa*, *p mirabilis* ,and week product biofilm in *S..haemolyticus*

Table 5 displays the antioxidant activity of two substances: TiO_2-NPs and the plant extract. The antioxidant activity is measured at different concentrations (µg/mL) for each substance. The green synthesized TiO_2-NPs generally exhibit higher antioxidant activity compared to plant extract across all concentrations. The antioxidant activity increases with the concentration for both green synthesized TiO_2-NPs and plant extract, suggesting a dose-dependent relationship. The TiO_2-NPs appear to enhance the antioxidant activity of plant extract, as evidenced by higher percentages at each concentration compared to the plant extract alone. The highest antioxidant activity is observed at the highest concentration (200 µg/mL) for both green synthesized TiO_2-NPs and plant extracts. This data suggests that the green synthesized TiO_2-NPs may have a synergistic effect on antioxidant activity, providing a potentially more potent antioxidant formulation compared to the plant extract. In addition, it is worth mentioning that many studies have dedicated different activities to nanoparticles derived from microorganisms [20-24], while others dedicated those from plant extract [25-29]. However, among all living organisms, plants exhibit the most promising capacity for nanoparticle biosynthesis, making them well-suited for extensive biosynthetic processes. In contrast to microorganisms, the production of nanoparticles derived from plants is characterized by greater speed and enhanced stability [30].

CONCLUSION

The results of this study demonstrate that the production of TiO_2-NPs by the green synthesis approach yielded nanoparticles with consistent stability, and these were characterized by their physicochemical characteristics of chemical compositions, shape and size. Most of the isolates that were used in present study high antibiotic resistance in most of the antibiotic classes that reached 100%.s.*haemolyticus*,*sepidermids*,*p. mirabilis*,and *p.aeruginosa* isolates the ability to produce biofilm in four levels of intensity: strong, moderate, weak, and non-biofilm-producing. The MIC can reduce the biofilm formation of isolated from urinary tract infections. TiO_2-NPs when presented as a homogenized blend exhibited robust anticancer potential and yielded the maximum antioxidant activity, demonstrating robust and necessary anticancer ability against the skin cancer cell line, which helped to overcome the cell cancer cells. The observations suggested that the TiO_2-NPs may impaled as a future therapeutic anticancer cure. The effects on both anticancer and antioxidant activity can be associated with both the direct influence of the TiO_2-NPs, as well as the indirect effects via the antioxidant capacity of the TiO_2-NPs in supporting to combat cancer.

ACKNOWLEDGMENT

The authors wish to express their genuine gratitude to the Department of Applied Science Laboratories, University of Technology, (Baghdad/ Iraq) for its experimental aid.

CONFLICT OF INTEREST

The authors declare that there are no conflicts of interest regarding this article.

REFERENCES

1. Bogdan J, Pławińska-Czarnak J, Zarzyńska J. Nanoparticles of Titanium and Zinc Oxides as Novel Agents in Tumor Treatment: a Review. Nanoscale research letters.

2017;12(1):225-225.
2. Drug Discovery and Evaluation: Methods in Clinical Pharmacology: Springer Berlin Heidelberg; 2011.
3. Malik S, Muhammad K, Waheed Y. Nanotechnology: A Revolution in Modern Industry. Molecules (Basel, Switzerland). 2023;28(2):661.
4. Das B, Tripathy S, Adhikary J, Chattopadhyay S, Mandal D, Dash SK, et al. Surface modification minimizes the toxicity of silver nanoparticles: an in vitro and in vivo study. JBIC Journal of Biological Inorganic Chemistry. 2017;22(6):893-918.
5. Avolio R, D'Albore M, Guarino V, Gentile G, Cocca MC, Zeppetelli S, et al. Pure titanium particle loaded nanocomposites: study on the polymer/filler interface and hMSC biocompatibility. Journal of Materials Science: Materials in Medicine. 2016;27(10).
6. Shoaib M, Saeed A, Rahman MSU, Naseer MM. Mesoporous nano-bioglass designed for the release of imatinib and in vitro inhibitory effects on cancer cells. Materials Science and Engineering: C. 2017;77:725-730.
7. Bonan RF, Mota MF, da Costa Farias RM, da Silva SD, Bonan PRF, Diesel L, et al. In vitro antimicrobial and anticancer properties of TiO2 blow-spun nanofibers containing silver nanoparticles. Materials Science and Engineering: C. 2019;104:109876.
8. Hariharan D, Thangamuniyandi P, Jegatha Christy A, Vasantharaja R, Selvakumar P, Sagadevan S, et al. Enhanced photocatalysis and anticancer activity of green hydrothermal synthesized Ag@TiO_2 nanoparticles. J Photochem Photobiol B: Biol. 2020;202:111636.
9. Boskabady MH, Tabatabayee A, Amiri S, Vahedi N. The effect of vitamin E on pathological changes in kidney and liver of sulphur mustard-exposed guinea pigs. Toxicology and Industrial Health. 2011;28(3):216-221.
10. Shanavas S, Priyadharsan A, Karthikeyan S, Dharmaboopathi K, Ragavan I, Vidya C, et al. Green synthesis of titanium dioxide nanoparticles using Phyllanthus niruri leaf extract and study on its structural, optical and morphological properties. Materials Today: Proceedings. 2020;26:3531-3534.
11. ÇElİKsÖZ M, Ulus B, ÖZtaŞ E, ÖZhan G. Diclofop-methyl: A phenoxy propionate herbicide with multiple toxic effects in mouse embyro fibroblast (NIH/3T3) cell line. Marmara Pharmaceutical Journal. 2017;21(4):992-997.
12. Elshikh M, Ahmed S, Funston S, Dunlop P, McGaw M, Marchant R, Banat IM. Resazurin-based 96-well plate microdilution method for the determination of minimum inhibitory concentration of biosurfactants. Biotechnology letters. 2016;38(6):1015-1019.
13. Shinde S, Lee LH, Chu T. Inhibition of Biofilm Formation by the Synergistic Action of EGCG-S and Antibiotics. Antibiotics (Basel, Switzerland). 2021;10(2):102.
14. Rao GT, Stella RJ, Babu B, Ravindranadh K, Venkata Reddy C, Shim J, Ravikumar RVSSN. Structural, optical and magnetic properties of Mn2+ doped ZnO-CdS composite nanopowder. Materials Science and Engineering: B. 2015;201:72-78.
15. Hasoon BA, Hasan DMA, Jawad KH, Shakaer SS, Sulaiman GM, Hussein NN, et al. Promising antibiofilm formation: Liquid phase pulsed laser ablation synthesis of Graphene Oxide@Platinum core-shell nanoparticles. PLoS One. 2024;19(9):e0310997-e0310997.
16. Torres A, Vargas Y, Uribe D, Carrasco C, Torres C, Rocha R, et al. Pro-apoptotic and anti-angiogenic properties of the α /β-thujone fraction from Thuja occidentalis on glioblastoma cells. Journal of Neuro-Oncology. 2016;128(1):9-19.
17. Biswas R, Mandal SK, Dutta S, Bhattacharyya SS, Boujedaini N, Khuda-Bukhsh AR. Thujone-Rich Fraction of Thuja occidentalis Demonstrates Major Anti-Cancer Potentials: Evidences from In Vitro Studies on A375 Cells. Evidence-based complementary and alternative medicine : eCAM. 2011;2011:568148-568148.
18. Sunila ES, Kuttan G. A Preliminary Study on Antimetastatic Activity of Thuja Occidentalis L. in Mice Model. Immunopharmacology and Immunotoxicology. 2006;28(2):269-280.
19. Saha S, Bhattacharjee P, Mukherjee S, Mazumdar M, Chakraborty S, Khurana A, et al. Contribution of the ROS-p53 feedback loop in thuja-induced apoptosis of mammary epithelial carcinoma cells. Oncol Rep. 2014;31(4):1589-1598.
20. Hussein N, Khadum MM. Evaluation of the Biosynthesized Silver Nanoparticles'' Effects on Biofilm Formation. Journal of Applied Sciences and Nanotechnology. 2021;1(1):23-31.
21. Jabbar R, Hussein N. Evaluation The Antibacterial Activity of Biosynthesis Silver Nanoparticles by Lactobacillus Gasseri Bacteria. Journal of Applied Sciences and Nanotechnology. 2021;1(3):86-95.
22. Hikmet R, Hussein N. The Biological Activity of Mycosynthesized Silver Nanoparticles Against some Pathogenic Bacteria. Journal of Applied Sciences and Nanotechnology. 2022;2(1):59-68.
23. Abdul-Jabbar AM, Hussian NN, Mohammed HA, Aljarbou A, Akhtar N, Khan RA. Combined Anti-Bacterial Actions of Lincomycin and Freshly Prepared Silver Nanoparticles: Overcoming the Resistance to Antibiotics and Enhancement of the Bioactivity. Antibiotics (Basel, Switzerland). 2022;11(12):1791.
24. Hussein K. Detection of the antimicrobial activity of silver nanoparticules biosynthesized by streptococcus pyogenes bacteria. iraqi journal of agricultural sciences. 2020;51(2):500-507.
25. Ceylan S, Yardımcı ŞS, Camadan Y, Saral Ö, Özsen Batur Ö. Chemical composition of essential oil by SPME and evaulation antimicrobial, antioxidant activities of medicinal plant of Quercus infectoria galls. Acta Scientiarum Polonorum Hortorum Cultus. 2021;20(6):93-103.
26. Nguyen NTT, Nguyen TTT, Nguyen DTC, Tran TV. Green synthesis of $ZnFe_2O_4$ nanoparticles using plant extracts and their applications: A review. Science of The Total Environment. 2023;872:162212.
27. Bordiwala RV. Green synthesis and Applications of Metal Nanoparticles.- A Review Article. Results in Chemistry. 2023;5:100832.
28. Fan J, Yu H, Lu X, Xue R, Guan J, Xu Y, et al. Overlooked Spherical Nanoparticles Exist in Plant Extracts: From Mechanism to Therapeutic Applications. ACS Applied Materials and Interfaces. 2023;15(7):8854-8871.
29. Berhe MG, Gebreslassie YT. Biomedical Applications of Biosynthesized Nickel Oxide Nanoparticles. International journal of nanomedicine. 2023;18:4229-4251.
30. Khan N, Ali S, Latif S, Mehmood A. Biological Synthesis of Nanoparticles and Their Applications in Sustainable Agriculture Production. Natural Science. 2022;14(06):226-234.